Soil–Reinforcement Interaction: Effect of Reinforcement Spacing and Normal Stress

Amr M. Morsy[1]; Jorge G. Zornberg, F.ASCE[2]; Dov Leshchinsky, M.ASCE[3]; and Jie Han, F.ASCE[4]

Abstract: This paper presents, evaluates, and discusses experimental results of soil–reinforcement interaction tests conducted using a new device developed to assess the mechanical interaction between soil and reinforcement considering varying reinforcement vertical spacings. The experiments involved testing a geosynthetic-reinforced soil mass with three reinforcement layers: one was actively tensioned and the two neighboring layers were passive. Shear stresses from the actively tensioned reinforcement were conveyed to the passive reinforcement layers through the intermediate soil medium. Soil-reinforcement interaction tests were conducted with varying reinforcement vertical spacings and normal stresses. The load conveyed to the neighboring reinforcement layers was found to increase with increasing load in the actively tensioned reinforcement layer. The magnitude of load transfer was found to increase with decreasing vertical spacing, while the normal stress was determined to have a negligible effect on the magnitude of load transfer for the case of active loads representative of working stress conditions. However, since the soil–reinforcement interface strength decreases with decreasing normal stress, the magnitude of load transfer was observed to decrease with decreasing normal stresses for comparatively large active loads. **DOI: 10.1061/(ASCE)GT.1943-5606.0002180.** © *2019 American Society of Civil Engineers.*

Author keywords: Soil–reinforcement; Interface interaction; Reinforced soil; Geosynthetics; Reinforcement spacing.

Introduction

The interaction between soil and reinforcement plays a vital role in the load transfer between these two dissimilar materials, which could be considered to form a composite material that is able to resist externally applied loads (Palmeira 2009). The spacing between reinforcement layers governs the degree of interaction not only between the reinforcement and surrounding soil, but also between the soil–reinforcement interfaces of adjacent reinforcement layers. This complex interaction governs the overall mechanical response of the reinforced soil mass. Reinforcement spacing has been reported to have a comparatively greater effect on reinforced soil mass behavior than on the reinforcement tensile properties. This observation was reported for cases where the reinforcement vertical spacing was comparatively small (Leshchinsky et al. 1994; Leshchinsky and Vulova 2001; Adams et al. 2011; Morsy 2017; Morsy et al. 2017a, b; Shen et al. 2019).

Leshchinsky et al. (1994) conducted an experimental testing program on geosynthetic-reinforced soil unit cells to study the effect of reinforcement vertical spacing. They developed a device to visualize the displacement fields within a reinforced soil unit cell during pullout of single and double reinforcement layers. The sidewalls of both devices consisted of transparent Plexiglas to enable direct visualization of soil movement as the reinforcement tension load increased. The results of tests conducted with a single reinforcement layer showed that the shear stresses generated at the soil–reinforcement interface propagated away from the interface, forming a sheared zone around the reinforcement, often referred to as the shear band. The thickness of this zone was found to be independent of normal stress applied to the reinforced soil. The results of tests conducted with double reinforcement layers indicated that the pullout resistance was practically the same as that obtained from tests conducted with single reinforcement layers of the same length and under the same testing conditions. Leshchinsky et al. (1994) observed that the soil between reinforcement layers stiffened, causing the reinforcement layers and the soil mass in between them to behave as a monolithic block. This block involved two outer reinforcement interfaces on which shear stresses developed against the adjacent soil, while no shear displacements were observed to have developed on the two interfaces adjacent to the stiffened soil block (i.e., no shear stresses were generated at the inner interfaces). However, this behavior was found to occur only at comparatively high normal stresses.

Leshchinsky et al. (1994) also reported that the failure surface is unlikely to develop within the reinforced soil mass when reinforcements of typical stiffness and strength are closely spaced. Instead, the failure surface developed behind the reinforced soil zone. Closely spaced reinforcements resulted in the formation of a composite material that behaved as a monolithic mass. Leshchinsky and Vulova (2001) conducted a subsequent study to evaluate the effects of vertical reinforcement spacing numerically. This numerical study adopted a moving reference algorithm in which deformation was allowed during construction and the height of the wall was numerically simulated to increase until a prevailing mode of failure

[1]Assistant Professor, Dept. of Civil Engineering, Cairo Univ., Giza 12613, Egypt; Geotechnical Engineer, Parsons Corporation, 301 Plainfield Rd., Syracuse, NY 13212; formerly, Graduate Research Assistant, Univ. of Texas at Austin, Austin, TX 78712 (corresponding author). ORCID: https://orcid.org/0000-0002-9335-7847. Email: amr.morsy@eng.cu.edu.eg

[2]Professor and W. J. Murray, Jr. Fellow in Engineering, Dept. of Civil, Architectural, and Environmental Engineering, Univ. of Texas at Austin, Austin, TX 78712.

[3]Professor Emeritus, Dept. of Civil and Environmental Engineering, Univ. of Delaware, Newark, DE 19716; Consultant, ADAMA Engineering, 12042 SE Sunny Rd., Clackamas, OR 97015.

[4]Glenn L. Parker Professor, Dept. of Civil, Environmental, and Architectural Engineering, Univ. of Kansas, Lawrence, KS 66045. ORCID: https://orcid.org/0000-0003-3137-733X

Note. This manuscript was submitted on December 12, 2018; approved on July 31, 2019; published online on October 3, 2019. Discussion period open until March 3, 2020; separate discussions must be submitted for individual papers. This paper is part of the ***Journal of Geotechnical and Geoenvironmental Engineering***, © ASCE, ISSN 1090-0241.

developed. Leshchinsky and Vulova (2001) concluded that, based on the numerical predictions, the reinforcement vertical spacing plays a major role in wall behavior and can significantly affect the prevailing mode of failure. They reported that the failure surfaces tended to develop behind the reinforced soil zone, with comparatively small reinforcement vertical spacing resulting in behavior that could be characterized as that of a composite material.

Failure of frictional materials is often characterized by localized deformations along failed zones, often referred to as shear bands. Shear bands can be characterized by certain thicknesses and patterns (Muhlhaus and Vardoulakis 1987; Alshibli and Sture 1999; Chen et al. 2008; Costa et al. 2009; Iglesias et al. 2013; Rui et al. 2016), which depend on the type of failure that develops in a soil system. Specifically, a shear band can be characterized by its thickness and general geometry. The thickness of a shear band increases with increasing shear strain. Beyond interface shear strength yield, shear strains in these bands are generally plastic and accommodate most of the additional deformation. Extensive research has been conducted to analyze and quantify the mechanisms leading to the development of shear bands in soils. More recent studies have focused on the development of shear bands at the interface of geosynthetic-reinforced soil systems (e.g., Fannin and Raju 1993; Zhou et al. 2012; Morsy et al. 2017a, b, 2018, 2019; Zornberg et al. 2019).

Ketchart and Wu (2001, 2002) investigated the behavior of geosynthetic-reinforced soil masses under various loading conditions. The study aimed at developing a simplified analytical model to predict the deformation characteristics of a generic geosynthetic-reinforced soil mass. The researchers developed a soil–geosynthetic interaction laboratory test aimed at capturing the interaction between the backfill soil and geosynthetic reinforcement. The test involved applying a vertical load on a geosynthetic-reinforced soil mass under plane strain conditions. The applied load was observed to transfer from soil to geosynthetic, allowing both materials to deform in an interactive manner. A similar study was conducted by Jacobs et al. (2013), in which a large-scale device was developed to investigate the behavior of geosynthetic-reinforced soil masses tested under plane strain conditions and subjected to vertical compression and constant lateral confining pressures. The device included a transparent sidewall to facilitate identifying the effect of the reinforcement on the kinematic behavior of soil, which allowed investigation of the load transfer between reinforcements and soils based on the development of the shear zone.

Overall, geosynthetic-reinforced structures may exhibit different behaviors when reinforcement spacing changes. However, the reinforcement spacing at which significant change in behavior occurs between what is referred to as closely spaced reinforced soil and largely spaced reinforced soil has not yet been defined based on a mechanical phenomenon. To evaluate the effect of reinforcement spacing and normal stress on soil–reinforcement interaction, a comprehensive testing program was conducted in this study using the experimental approach and equipment detailed in Morsy (2017). Specifically, the new soil–geosynthetic interaction device was used to quantify the displacements along the length of an active reinforcement layer, the relative displacements along the soil–reinforcement interface, the displacements field within the soil mass in the vicinity of the active reinforcement layer, and the displacements along the length of two reinforcement layers placed adjacent to the active layer at varying vertical spacings. The testing program was designed to evaluate test repeatability and the effect of reinforced soil normal stress and reinforcement vertical spacing on the soil–reinforcement interaction. This paper also discusses the results of a parametric evaluation considering these variables.

Experimental Approach

A new experimental device, shown in Fig. 1, was designed and developed at the University of Texas at Austin to evaluate the soil–reinforcement interaction and quantify the thickness of the soil shear band that develops near the soil–reinforcement interface upon shear stress generation (Morsy 2017; Morsy et al. 2019). The box was designed to accommodate soil specimens up to 1,200 mm deep, 150 mm long, and 750 mm wide. Six pneumatic actuators were placed on wooden pyramids that covered the top surface of the reinforced soil mass reacting against a stiff reaction frame, which conveyed the reaction load exerted by the actuators to the bottom of the box. This normal pressure system was designed to assess soil dilatancy. Additionally, this system maintained a controlled-dilation condition to allow for the comparison of the soil–reinforcement interaction in free, reduced, and suppressed soil-dilation conditions. The axial loading system consisted of two hydraulic actuators reacting against the front wall of the box. The loading system was connected to a clamping system that conveyed the applied tensile load to the active reinforcement. The embedded reinforcement layer was subjected to increasing loads, with particular focus on the responses under loads representative of working stress and ultimate stress conditions. In addition to the active reinforcement layer, two additional passive reinforcement layers of the same type were used as upper and lower boundaries to represent the presence of contiguous reinforcements. To properly model the behavior of the passive reinforcements, soil was placed between the passive reinforcements and the top and bottom boundaries of the box. A combination of collars (to heighten the box) was used to control the soil thickness.

A schematic layout of the testing device used in this study is presented in Fig. 1(a). Many of its characteristics were based on those of large-scale pullout devices. A distinctive feature of this experimental system is its ability to accommodate multiple reinforcement layers at different vertical spacings, as shown in Fig. 1(b). Specifically, the device included a geosynthetic-reinforced soil mass containing three reinforcement layers: one reinforcement layer was placed at the midheight of the soil mass and actively loaded during the test; and two neighboring reinforcement layers were passive during the test. It should be noted that the experimental device is not intended to simulate a prototype structure; instead, the device represents a unit reinforced soil mass involving an actively loaded reinforcement and two neighboring passive reinforcements. Ultimately, the device allows the unevenly loaded contiguous reinforcements to be investigated. This in turn allows the evaluation of the interaction of multiple loaded reinforcement layers in a reinforced soil mass. This device parts the interaction of every single reinforcement layer with its adjacent soil and neighboring reinforcement layers from the global reinforced soil system in which all reinforcement layers work together. It should also be noted that the findings reached from the experimental program conducted in this study can be extended to any multilayered geosynthetic-reinforced soil mass.

The device was extensively instrumented to provide a comprehensive evaluation of the reinforced soil mass behavior, including: (1) the effect of the shear stress generated by one of the reinforcement layers (i.e., active reinforcement) on adjacent reinforcement layers; (2) the straining of geosynthetic reinforcements; (3) the evolution of the shear band near the soil–reinforcement interface; (4) the stiffness of the soil–reinforcement interface; (5) the unit tension in the reinforcement at working stress and ultimate stress levels; and (6) the dilatancy in the reinforced soil mass upon shear stress mobilization at the soil–reinforcement interface when volume changes are allowed.

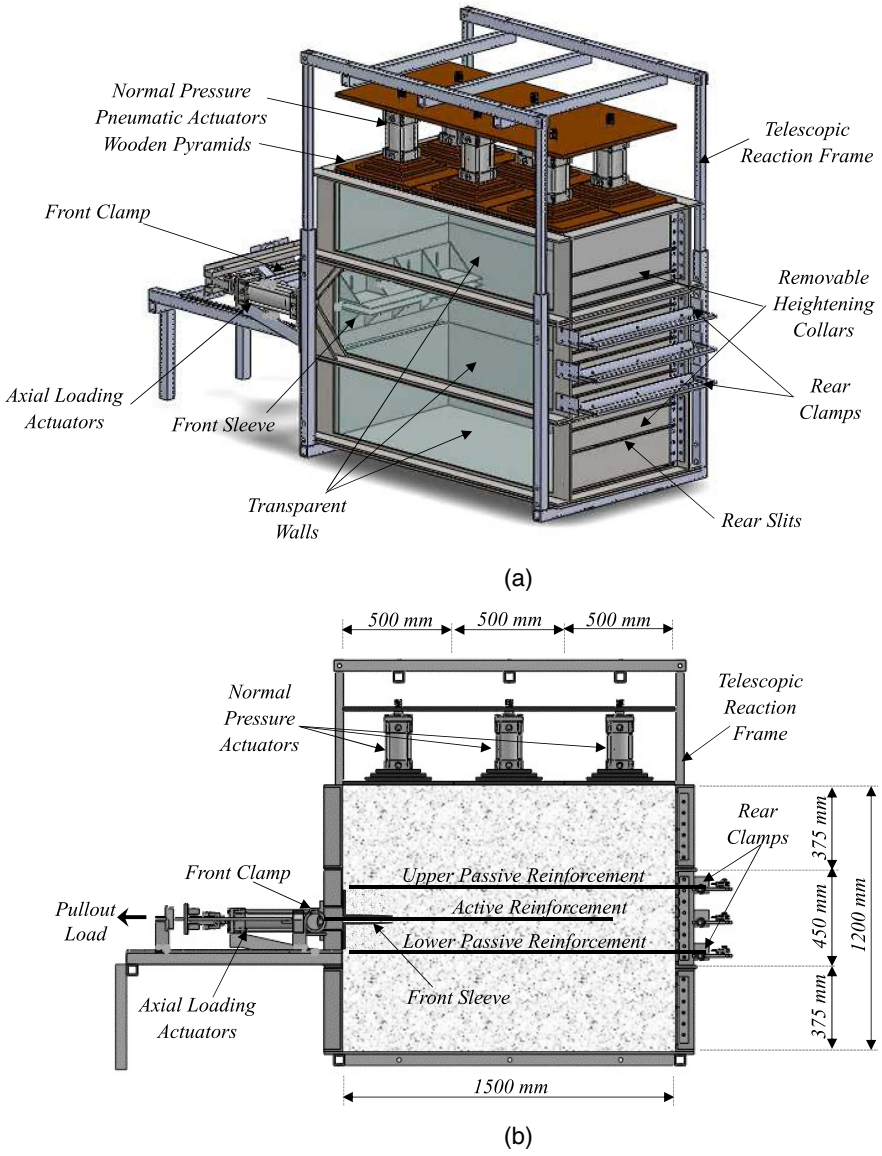

Fig. 1. Soil–geosynthetic interaction device: (a) general layout; and (b) schematic sectional side view.

The instrumentation adopted in the soil–geosynthetic interaction device included: (1) a load cell to measure the tensile load applied to the active reinforcement; (2) load cells at the pneumatic actuators to monitor the actual normal pressure applied on top of the reinforced soil mass throughout testing; (3) displacement sensors to measure displacements at multiple locations within the active and passive reinforcements, as shown in Fig. 2 (u1 through u10 for the active reinforcement; v1 through v5 for the upper passive reinforcement; and w1 through w5 for the lower passive reinforcement); (4) artificial gravel-size particles buried within the soil mass, as shown in Fig. 3 (x1 through x9) and connected to displacement sensors via horizontal telltales, facilitating measurement of internal displacements; and (5) artificial gravel-size particles placed on the surface of the reinforced soil mass (y1 through y3, as shown in Fig. 3) and connected to displacement sensors via vertical telltales to measure vertical displacements and to assess the dilatancy angle of the reinforced soil mass. A detailed description of the testing equipment and instrumentation is presented in Morsy (2017) and Morsy et al. (2019).

Testing Program

This section describes the testing scheme adopted in this study, while the subsequent sections detail the testing configurations for the various tests and characteristics of the materials used in the testing program. The equipment was designed to allow two configurations: (1) a 450 mm-high configuration, measuring 1,500 mm (L) × 300 mm (W) × 450 mm (H); and (2) a 1,200 mm-high configuration, measuring 1,500 mm (L) × 300 mm (W) × 1,200 mm (H). Three reinforcement layers were placed at vertical spacings ranging from 0.05 to 0.15 m for the first configuration and from 0.20 to 0.40 m for the second configuration. The target normal pressure at the active (i.e., middle) reinforcement layer ranged from 15 to 50 kPa. This normal pressure was intended to be low enough to allow pullout failure to occur before reinforcement rupture, thus allowing comparatively high deformations to develop in the reinforcement and surrounding soil without reaching tensile failure of the active reinforcement (i.e., reaching pullout failure instead). This facilitated understanding of the soil–reinforcement load-transfer mechanisms and an assessment of soil–reinforcement interaction

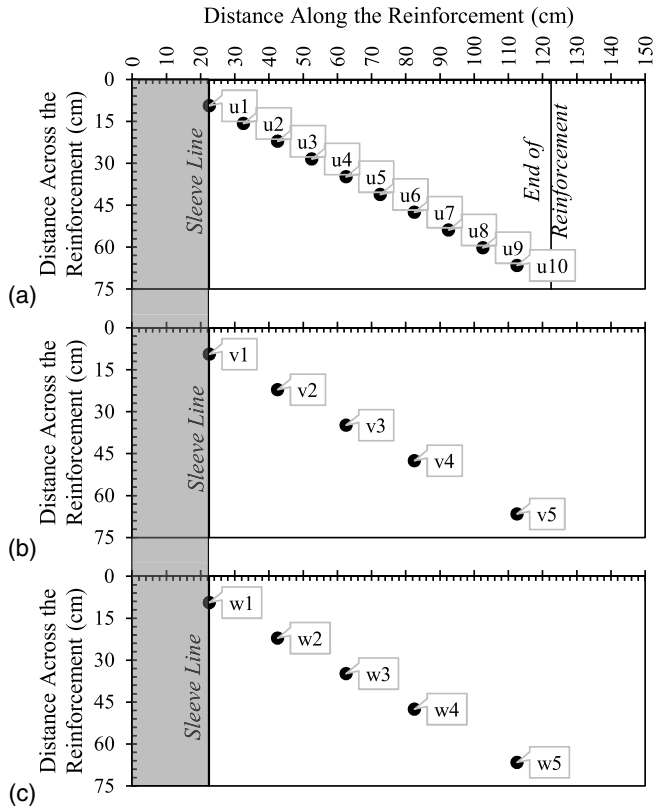

Fig. 2. Locations of telltale connections: (a) active reinforcement layer; (b) upper passive reinforcement layer; and (c) lower passive reinforcement layer.

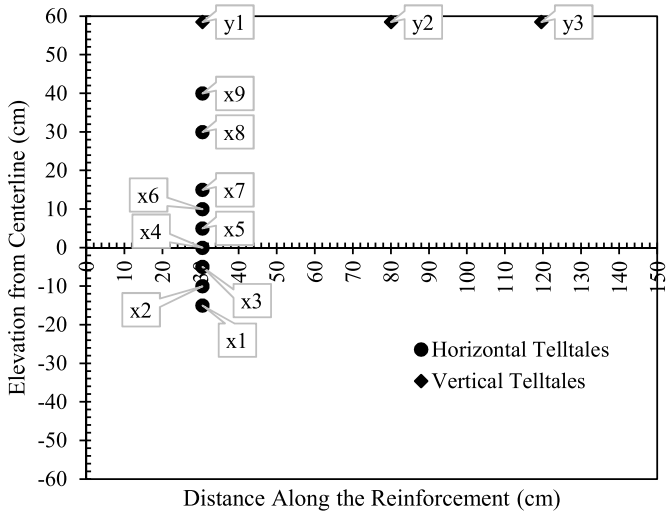

Fig. 3. Locations of artificial gravel particles within the reinforced soil mass. Particles at x8 and x9 exist only in the 1,200 mm configuration; and Particles at y1, y2, and y3 are located at elevation +21 cm in the 450 mm configuration.

behavior. The embedment length of the active reinforcement layer was 1,016 mm while the passive reinforcement layers were extended to the rear of the reinforced soil mass, where they were clamped. All reinforcement layers were straightened out and placed in the box with no preload.

Material Properties

This section presents the properties of the materials used in the testing program of the experimental component of the study.

Fill Material

The fill material used in most of the tests in this study was washed river pea gravel deposited by the Colorado River near Austin, Texas. This material is a uniformly graded clean gravel that classifies as GP (poorly graded gravel) according to the Unified Soil Classification System (USCS) [ASTM D2487 (ASTM 2017a)] and as A-1-a according to American Association of State Highway and Transportation Officials (AASHTO) classification [AASHTO M145 (AASHTO 2017)]. The gravel gradation conforms to the standard range of AASHTO No. 8 grain size distribution. The material has subrounded to subangular particles and consists predominantly of quartz with traces of other minerals. The grain size ranges from approximately 1 to 13 mm, with a mean grain size of 7 mm.

The coefficients of uniformity and curvature for AASHTO Gravel No. 8 are 1.6 and 0.9, respectively. Its specific gravity is 2.62 [ASTM D854 (ASTM 2014)] and its maximum and minimum void ratios are 0.73 and 0.50, respectively. The corresponding maximum and minimum dry unit weight values are 15.14 and 17.47 kN/m^3, respectively. These values were determined in accordance with ASTM D4253 (ASTM 2016a) and ASTM D4254 (ASTM 2016b), respectively. The backfill material was placed in 75 mm-thick lifts and gently hand tamped until it reached a relative density of 70%, which corresponds to a dry unit weight of 16.67 kN/m^3 and a void ratio of 0.57.

The shear strength of the backfill used in this study was evaluated through a set of triaxial tests on specimens measuring 152.4 mm in diameter and 330.2 mm in height. Three tests were conducted at three different confining stress levels of 35, 70, and 105 kPa and a relative density of 70%. The peak friction angle was 36.9° with a cohesion intercept of 15.6 kPa for the range of confining stresses tested. In addition to the characterization of the fill material using triaxial tests, an additional series of tests was conducted using a large-scale direct shear device, designed to accommodate soil samples with particles up to 25 mm. The direct shear testing program conducted in this study met the following general criteria: (1) the width of the direct shear box exceeded 10 times the maximum particle size [ASTM D3080 (ASTM 2011)]; and (2) the width-to-thickness (B:H) ratio of the direct shear box exceeded 2:1. The direct shear specimens tested in the experimental program had a length and width of 510 mm and a height of 200 mm. Tests were conducted at normal stress levels of 10.5, 21, and 35 kPa on specimens prepared at a relative density of 70%. The peak friction angle was 37.6° with a zero cohesion intercept for the range of normal stresses tested. Note that the focus of this study is on the load transfer from one reinforcement to other neighboring reinforcements through the enclosed soil media (i.e., further away from the actively loaded reinforcement layer). This load transfer depends on the properties of the transferring medium (i.e., soil). Thus, triaxial testing was found to be a reasonable method to conduct on the fill material to identify soil compressive and shear stiffness.

Reinforcement Material

The reinforcement was a woven geotextile, which has been commonly adopted in US practice for the case of geosynthetic-reinforced soil structures involving a comparatively small reinforcement spacing. The embedment length of the active reinforcement

J. Geotech. Geoenviron. Eng., 2019, 145(12): 04019115

Table 1. Reinforcement tensile properties

Mechanical property	Minimum average roll value (MARV)	
	Machine direction	Cross-machine direction
Ultimate tensile strength	70.0 kN/m @ 10% Strain	70.0 kN/m @ 8% Strain
Tensile strength at 2% strain	14.0	19.3
Tensile strength at 5% strain	35.0	39.4
Tensile strength at 10% strain	70.0	Not applicable

layer was 1,016 mm. The passive reinforcement layers were extended to the end of the reinforced soil mass, where they were clamped. The reinforcement material was a polyester woven geotextile commercialized under the name of HP570. This geotextile has multifilament yarns oriented in the rollway direction (i.e., machine direction) and monofilament yarns oriented in the cross-rollway direction (i.e., cross-machine direction). The unconfined tensile properties reported by the geotextile manufacturer are summarized in Table 1. It was reported that the tensile strength properties were obtained in accordance with ASTM D4595 (ASTM 2017b).

Soil–Reinforcement Interface

A large-scale direct shear device, originally designed to test large soil samples with grain sizes up to 25 mm, was modified as part of this study to evaluate the soil–reinforcement interface shear behavior. An interface direct shear testing program was implemented to evaluate the interface shear behavior between the fill material (AASHTO Gravel No. 8) and the reinforcement (woven geotextile). Two displacement-controlled direct shear tests were performed on compacted-gravel specimens with an applied normal stress ranging from 24 to 52 kPa. The geosynthetic reinforcement was glued to a smooth board using a heavy-duty epoxy. The woven geotextile specimen was glued so that the cross-rollway direction (i.e., cross-machine direction) was oriented toward the shear direction (i.e., the same direction as in the soil–reinforcement interaction tests). The interface shear strength was characterized by a friction angle of 28.7° and zero adhesion.

Parametric Evaluation

The testing program was designed to evaluate test repeatability and the effect of normal stress and reinforcement vertical spacing on soil–reinforcement interaction; Table 2 presents a summary of the tests considered in the evaluation of each aspect. This section provides a discussion of the results and analyses of a parametric evaluation considering these variables.

Assessment of Repeatability of Test Results

To assess the repeatability of the tests in the new device, a comparison was conducted of the results from two identical specimens tested under the same conditions. Table 2 summarizes the properties of the tests involved in this test series. Specifically, the two tests were conducted using the same polyester woven geotextile reinforcement. Each test involved three reinforcement layers of the same type (one active and two passive), placed at a vertical spacing of 0.10 m. Gravel meeting AASHTO No. 8 specifications was used as fill material in both tests. The two tests were conducted under normal stress of 50 kPa at the active reinforcement level (i.e., central horizontal plane of the reinforced soil mass).

Table 2. Summary of tests

Testing scheme	Test ID	Testing variables	
		S_v (m)	σ_v (kPa)
Repeated tests	GP-04-07-G1-G	0.10	50
	GP-04-07-G1-G(R)		
Tests with different normal stress levels	GP-06-02-G1-G	0.15	15
	GP-06-03-G1-G		21
	GP-06-05-G1-G		35
	GP-06-07-G1-G		50
	GP-04-03-G1-G	0.10	21
	GP-04-07-G1-G		50
	GP-02-03-G1-G	0.05	21
	GP-02-07-G1-G		50
Tests with different reinforcement vertical spacings	GP-02-07-G1-G	0.05	50
	GP-04-07-G1-G	0.10	
	GP-06-07-G1-G	0.15	
	GP-08-07-G1-G	0.20	
	GP-12-07-G1-G	0.30	
	GP-16-07-G1-G	0.40	
	GP-02-03-G1-G	0.05	21
	GP-04-03-G1-G	0.10	
	GP-06-03-G1-G	0.15	

Note: All tests were conducted with AASHTO No. 8 fill material, geotextile active and passive reinforcements, and free allowed dilation (i.e., allowed volume change). Some tests are mentioned more than once in different testing schemes to show the extent of variation within each scheme.

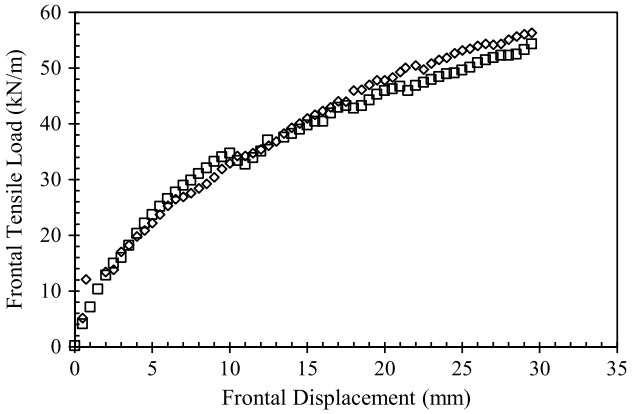

Fig. 4. Frontal tensile load-displacement curves.

The frontal load-displacement experimental curves for both tests showed good agreement, as presented in Fig. 4. Fig. 5 shows the displacement profiles for the active and passive reinforcement layers for the loading stages characterized by frontal displacements of the active reinforcement (u1) of 5, 10, 15, and 20 mm. A good match was observed between the displacement profiles obtained from both tests at the various loading stages, and a similar observation can be made regarding the displacement profiles of the passive reinforcement layers. Fig. 6 shows the horizontal soil displacement measured for nodal displacements of 5, 10, 15, and 20 mm, measured at specific locations via artificial gravel particles arranged within the soil in a vertical array 30.5 cm from the front wall. The soil displacements observed were also found to be very similar for both tests at the various loading stages.

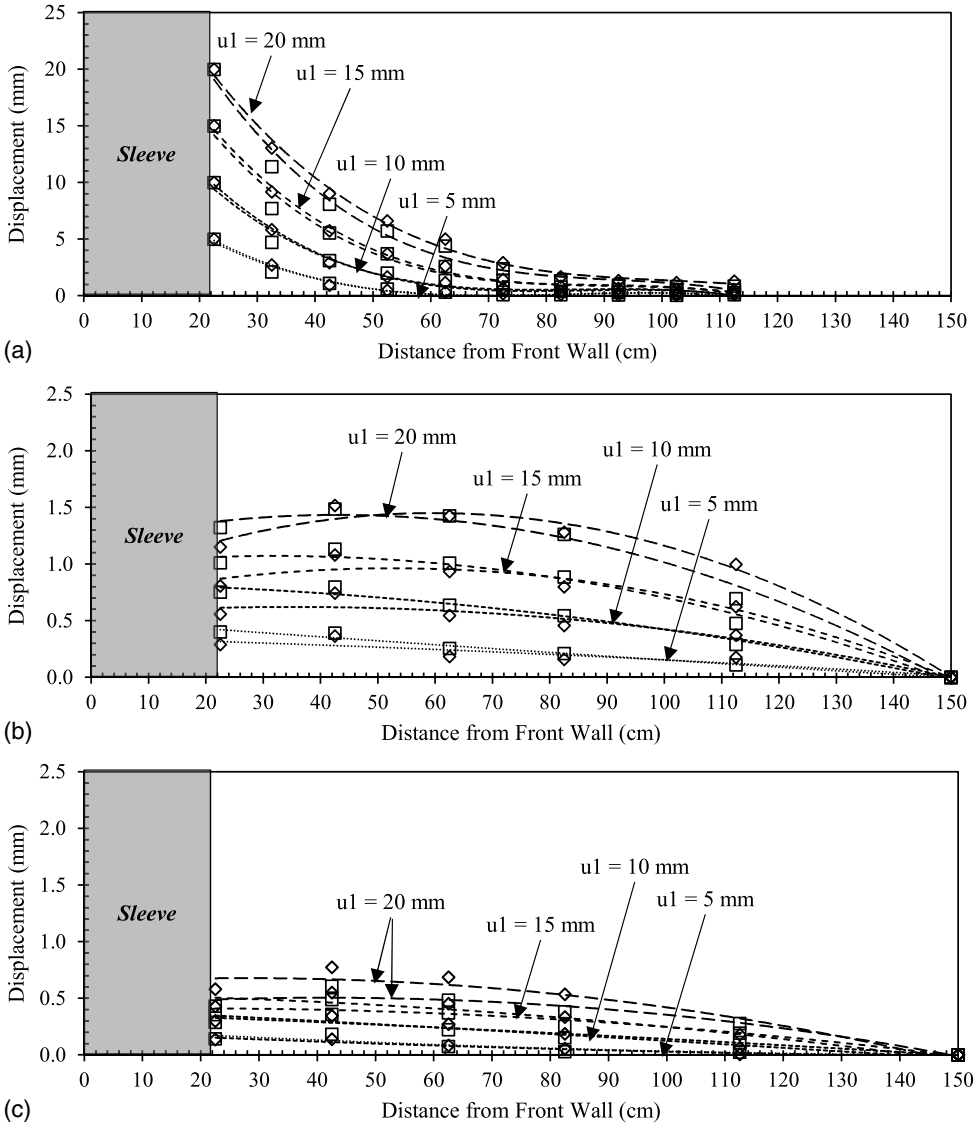

Fig. 5. Reinforcement displacement profiles at various frontal displacements u1: (a) active reinforcement; (b) upper passive reinforcement; and (c) lower passive reinforcement.

Effect of Normal Stress

To assess the effect of overburden pressure on the interaction between the contiguous reinforcement layers in geosynthetic-reinforced soil structures, a testing series was conducted involving the same testing configuration but at varied normal stress levels. Table 2 summarizes the characteristics of these tests, which allowed an assessment of the effect of normal stress on soil–geosynthetic interaction. This series consisted of four tests conducted with reinforcements spaced at 0.15 m, two tests conducted with reinforcements spaced at 0.10 m, and two tests conducted with reinforcements spaced at 0.05 m. The normal stress levels in these tests ranged from 15 to 50 kPa at the level of active reinforcement layer. This range was adopted so that most of the tests would fail in pullout, making it possible to assess the full range of soil–reinforcement interaction, including working stress and ultimate strength conditions.

Three comparisons among the results from tests conducted at various normal stress levels and different reinforcement vertical spacings were carried out: (1) a comparison of the results from four tests conducted at normal stresses of 15, 21, 35, and 50 kPa at the active reinforcement level, with reinforcements placed at a vertical spacing of 0.15 m; (2) a comparison of the results from two tests conducted at normal stresses of 21 and 50 kPa at the active reinforcement level, with reinforcements placed at a vertical spacing of 0.10 m; and (3) a comparison of results from two tests conducted at normal stresses of 21 and 50 kPa at the active reinforcement level, with reinforcements placed at a vertical spacing of 0.05 m. Tests in the same comparison group were conducted under the same testing conditions using the same reinforcement and fill materials. Specifically, the same polyester woven geotextiles and AASHTO No. 8 gravel were used in all tests. That is, among tests in the same comparison group, only the normal stress level differed.

Figs. 7(a–c) show the frontal tensile load-displacement experimental curves for the tests conducted with reinforcements placed at vertical spacings of 0.15, 0.10, and 0.05 m, respectively. The results indicate that the resistance of the active reinforcement to tensile load increased with increasing normal stress. This trend was the same for tests conducted with reinforcements placed at different vertical spacings. In addition, the soil–reinforcement interface shear strength was found to increase with increasing normal stress.

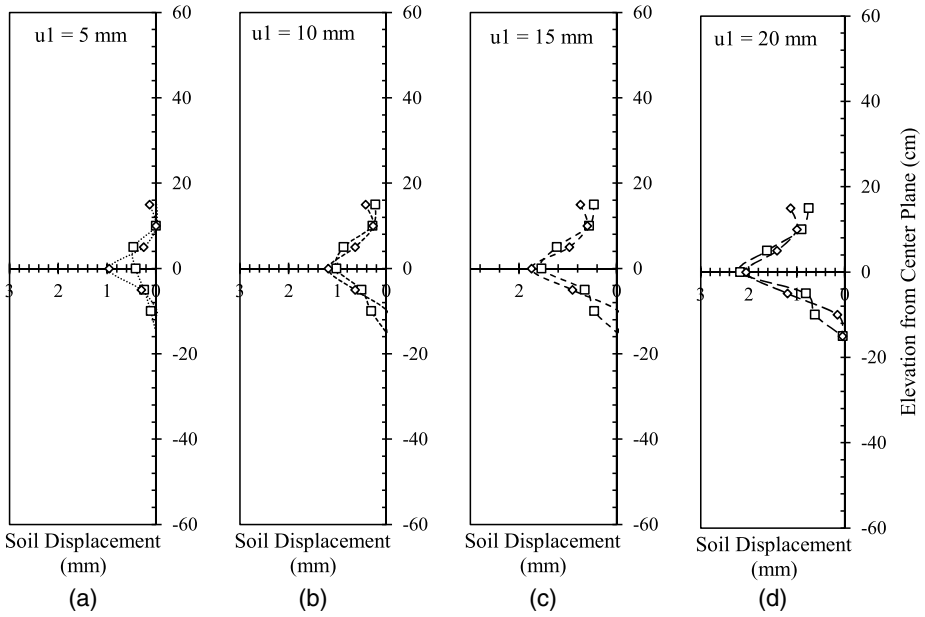

Fig. 6. Horizontal soil displacement profiles (measured via instrumented artificial gravel particles) at various frontal displacements u1: (a) u1 = 5 mm; (b) u1 = 10 mm; (c) u1 = 15 mm; and (d) u1 = 20 mm.

Figs. 8(a and b) present the average displacements for the upper and lower passive reinforcement layers, respectively, in relation to the average displacements of the active reinforcement layer for tests conducted with a reinforcement spacing of 0.15 m. Figs. 8(a and b) reflect the load transfer from the active reinforcement to the passive reinforcements at the same nodal reinforcement of the active reinforcement (i.e., the same soil–reinforcement interface shear displacement). The average displacement represents the area under the displacement profile normalized by the reinforcement length. Assuming the interface shear stress-displacement constitutive behavior is linear and of similar stiffness at the range of tested normal stresses, the trends shown in Figs. 8(a and b) provide insight into the effect of normal stress on the interaction between neighboring reinforcements. Note that the difference in the measurements between the upper and lower passive reinforcement layers is attributed to the difference in the overburden pressure above and below the active reinforcement layer. For tests conducted at a comparatively low normal stress (e.g., 15 kPa), the difference in overburden pressure was observed to cause differences in soil–reinforcement interaction behavior. The differences, however, are minor in tests conducted with comparatively large normal stresses (e.g., 50 kPa), in which the difference in overburden pressure represents a small fraction of the applied 50 kPa. In addition, the soil mass below the active reinforcement is bordered by a rigid floor, while the soil mass above the active reinforcement is bordered by a flexible normal pressure system. However, this aspect is expected to be minor compared to the effect of the overburden pressure discussed earlier. The difference in soil–reinforcement interaction behavior is minor in tests conducted with the tall configuration (1,400 mm depth) of the device as compared to the short configuration (450 mm depth).

The results indicate that the relationship between the displacements of the passive reinforcements and the active reinforcement is linear at early loading stages. This relationship then becomes nonlinear as the load-displacement relationship of the active reinforcement curves. That is, the results in Figs. 8(a and b) indicate the effect of the interface condition of the passive reinforcement on the interaction between the contiguous reinforcement layers. Specifically, at early loading stages, no significant difference was observed in the displacements in the passive reinforcements. However, as loading progressed, the soil–reinforcement interaction strength yielded more in the tests conducted under low normal stresses than in the tests conducted under high normal stresses. Overall, for the range considered in this experimental program, normal stress did not exhibit a significant effect on the degree of interaction between the active and passive reinforcement layers before the yielding of interface strength (i.e., under working stresses). However, the results also show that increasing normal stresses led to more significant interaction between contiguous reinforcements for the case of comparatively high interface shear stresses. This is because the higher interface strength resulting under comparatively high normal stresses yields at larger interface displacements. Furthermore, at high normal stresses, the soil (i.e., the medium allowing the shear stress transfer) is comparatively stiff and can more effectively transfer stresses before yielding either internally or at the soil–reinforcement interface. This observation corroborates the observation by Leshchinsky et al. (1994), in which a soil between reinforcement layers behaved compatibly with reinforcements as a monolithic at comparatively high confining stresses. Similar trends were obtained in the tests conducted with reinforcement layers spaced at 0.05 and 0.10 m.

Figs. 9(a–d) show the displacement profiles for the active and passive reinforcement layers spaced at 0.15 m at active reinforcement frontal displacements (u1) of 5, 10, 15, and 20 mm, respectively. This comparison is made for loading stages corresponding to the same frontal displacements (u1) of the active reinforcements, rather than the same frontal tensile loads applied on the active reinforcements. The profiles of tests conducted at low normal stress showed higher displacements along the length of the active reinforcement than those conducted at high normal stress. This difference increased as loading progressed (i.e., as values of u1 increased). The profiles of the passive reinforcement layers also showed higher displacement values for the tests conducted at low normal stress compared to those conducted at high normal stress. However, these differences tended to decrease and even reverse as frontal tensile loading progressed (i.e., as active reinforcement

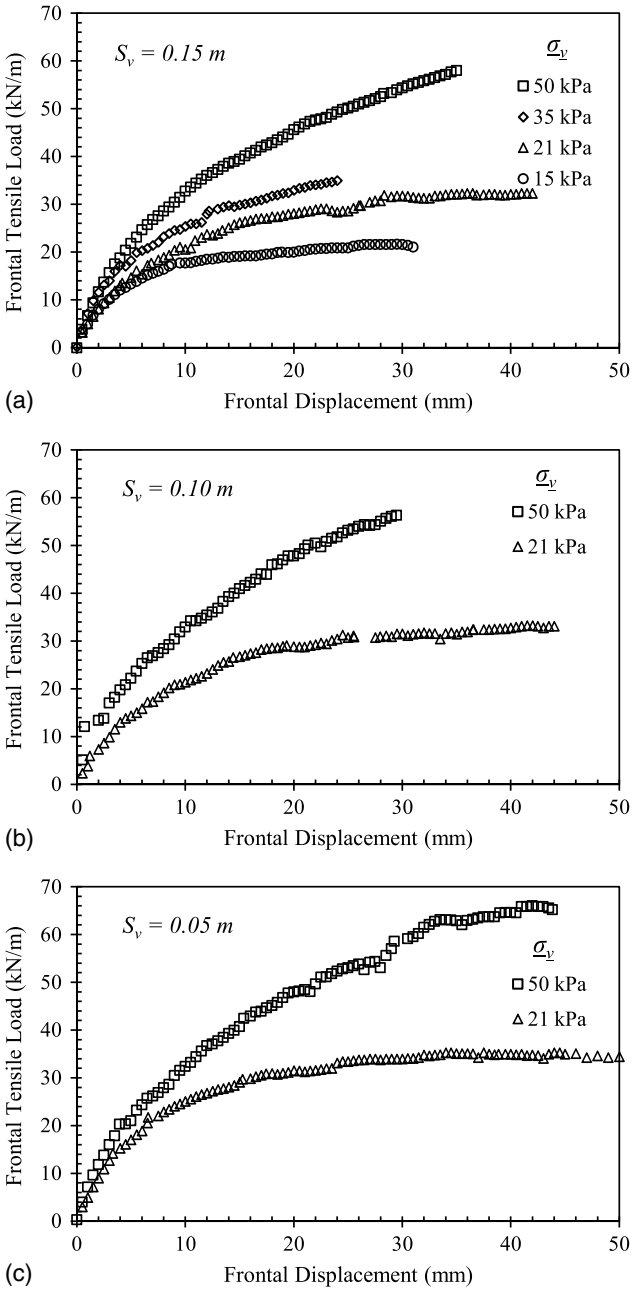

Fig. 7. Frontal tensile load-displacement curves: (a) tests conducted with $S_v = 0.15$ m; (b) tests conducted with $S_v = 0.10$ m; and (c) tests conducted with $S_v = 0.05$ m.

displaces, as illustrated by its displacement profiles). The reinforcement tested at low normal pressure could mobilize more soil to transfer load for the same frontal displacement value. That is, the effect of normal stress on the interaction between adjacent reinforcements cannot be revealed by comparing the displacement profiles of passive reinforcements at the same u1 values for tests conducted at different normal stresses. Similar trends were obtained in the tests conducted with reinforcement layers spaced at 0.05 and 0.10 m.

The upper passive reinforcement displacement profiles for the same integrated displacements of the active reinforcement (i.e., soil–reinforcement interface strength mobilization) were compared to provide a suitable assessment. Note that at working stress conditions, the relationship between mobilized interface strength and displacement is practically linear. That is, the integrated displacements of reinforcement at working stress conditions represent the integrated mobilized strengths because the soil–reinforcement interface stiffness is practically the same for displacements within working stress conditions. Consequently, comparisons were conducted for similar soil–reinforcement-induced reinforcement displacement to provide added insight into the ability of the adjacent reinforcements to interact at different normal stress levels considering the same soil and reinforcement materials. Higher interaction among reinforcement layers was observed at high normal stresses. Similar trends were obtained for test groups conducted with the reinforcement vertical spacings of 0.05, 0.10, and 0.15 m. In addition, varying the reinforcement spacings was found to have no impact on the effect of the normal stress magnitude on the reinforcement interaction.

Fig. 10 shows the vertical soil displacement measured via artificial gravel particles placed on top of the reinforced soil mass. Figs. 10(a–c) show the soil displacement in relation to the reinforcement frontal displacement of the active reinforcement u1 for the front, middle, and back of the reinforced soil mass, respectively. The results from tests conducted at normal stresses of 15, 21, and 35 kPa at the active reinforcement level are shown in the figures. The results indicate that the soil tended to dilate near the front and settle near the back as frontal tensile loading progressed. Dilation was found to be higher in tests conducted at low normal stresses than those conducted at high normal stresses. These trends are consistent with the increased dilatancy expected for decreasing normal stresses during soil shearing. Similar trends were obtained for the tests conducted using reinforcements placed at different reinforcement vertical spacings.

Effect of Reinforcement Vertical Spacing

Two sets of experimental tests were conducted to assess the effect of reinforcement vertical spacing on the behavior of a reinforced soil mass. Table 2 summarizes the conditions of the tests conducted as part of this series. All tests involved three reinforcement layers, one active and two passive. The same polyester woven geotextile was used in all tests as reinforcement, while AASHTO No. 8 gravel was used as fill material. Two comparisons were made among tests conducted at the same normal stress but with different reinforcement vertical spacings: (1) a comparison of six tests conducted at a normal stress of 50 kPa at the active reinforcement level; and (2) a comparison of three tests conducted at a normal stress of 21 kPa at the active reinforcement level. The findings of both comparisons were assessed against one another to evaluate the effect of normal stress on the trends observed for reinforcements placed at different vertical spacings within the reinforced soil mass.

Figs. 11(a and b) show the frontal load-displacement experimental curves for tests conducted at normal pressures of 50 and 21 kPa, respectively. A good match between the curves can be observed, particularly in the early loading stages. At higher loading levels, the agreement is still very good, although it shows comparatively higher scatter. This trend demonstrates that the reinforcement vertical spacing had a negligible effect on pullout resistance when using the woven geotextile as active and passive reinforcement. A minor difference in the maximum pullout resistance can be observed in Fig. 11(b), which compares the results of tests conducted at low normal stress (21 kPa). For the tests reported in Fig. 11(b), the reinforced soil tended to dilate more than in tests conducted at a higher normal pressure (50 kPa). The results indicate that the tendency for dilation was smaller for tests conducted using comparatively smaller reinforcement vertical spacing. That is,

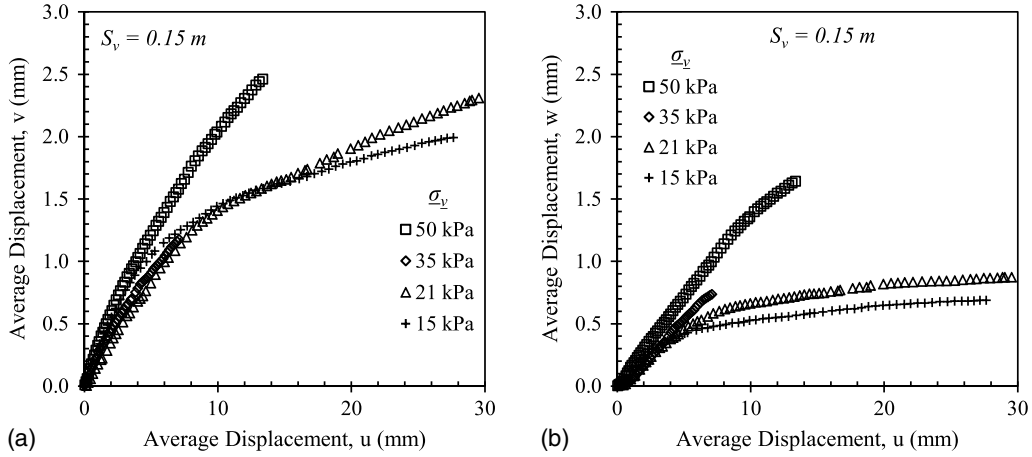

Fig. 8. Average displacements at the passive reinforcement layers relative to average displacements at the active reinforcement layer for tests conducted with $S_v = 0.15$ m: (a) upper passive reinforcement layer; and (b) lower passive reinforcement layer.

a decrease in vertical spacing resulted in reduced dilation in the reinforced soil mass, which is consistent with the effect on soil dilation of increased confinement and increased soil–reinforcement interaction strength.

Fig. 12 shows the average displacements measured in the active reinforcement and the corresponding average displacements in the passive reinforcements. Specifically, Figs. 12(a and b) show the average displacement of the upper and lower passive reinforcement layers, respectively, for tests conducted at normal stresses of 50 kPa, whereas Figs. 12(c and d) show the average displacement of the upper and lower passive reinforcement layers, respectively, for tests conducted at normal stresses of 21 kPa. The average displacement is the area under the displacement profile normalized by the reinforcement length. Assuming the constitutive behavior for interface shear behavior, Figs. 12(a–d) provide insight into the effect of normal stress on the interaction between adjacent reinforcements. The results indicate that larger reinforcement vertical spacing results in comparatively smaller interaction between adjacent reinforcements. The effect of reinforcement spacing was found to be more pronounced at high normal stresses.

Fig. 13 compares the interface shear strength back-calculated from the soil–geosynthetic interaction test results under ultimate conditions and that obtained from large-scale direct shear testing. The ultimate tensile load values for the tests conducted under normal stresses of 35 and 50 kPa were obtained by extrapolating the frontal tensile load-displacement curves. Because no trend for the ultimate pullout resistance values could be defined for tests conducted with reinforcements placed at different vertical spacings, the average values at normal stresses of 21 and 50 kPa were used to determine the interface strength envelope. The presented results provide the characteristic direct interface shear behavior for the reinforcement and fill materials used in this study. The results indicate that the interface friction angle obtained from the interpretation of soil–geosynthetic interaction test results (30.4°) was slightly higher than that obtained from direct shear testing (28.7°). This can be attributed to the additional passive resistance that can be mobilized in soil–geosynthetic interaction tests with comparatively flexible geotextiles. Forensic evaluation of the reinforcement layers after completion of testing revealed the presence of holes and intruding marks in the woven geotextile caused by the adjacent gravel particles. This type of interaction is somewhat similar to the passive-resistance contribution of transverse ribs in geogrid reinforcements. The comparison made in Fig. 13 is important to manifest the extent of passive resistance the geotextile asperity may add to the interface friction (i.e., the difference between pullout resistance and direct shear strength) for the reinforcement and fill materials used in this study.

The experimental data generated as part of this study is useful in addressing the question of what constitutes a reinforced soil mass with closely spaced reinforcements, i.e., the vertical reinforcement spacing below which the loading of a geosynthetic reinforcement affects the deformation response and load magnitude of adjacent reinforcement layers (Zornberg et al. 2019). Fig. 14 shows the experimental data useful in quantifying the effect of reinforcement vertical spacing on the interaction between adjacent reinforcement layers. The indicator adopted in this evaluation to quantify this interaction is the ratio between the reinforcement displacements measured in a passive reinforcement, v, to the corresponding displacement measured in the active reinforcement, u. Specifically, Figs. 14(a–c) show the ratio adopted as indicator (v/u) as a function of reinforcement vertical spacing for different stages or loading levels in a test (characterized by displacements in the active reinforcement of 2, 5, and 10 mm). Two inflection points can be observed in the relationships shown in the figures: (1) at a vertical spacing $S_{v,c}$ (i.e., composite threshold) below which full interaction occurs between adjacent reinforcements; and (2) vertical spacing $S_{v,nc}$ (i.e., noncomposite threshold) beyond which no interaction occurs between adjacent reinforcements. Varying degrees of interaction between adjacent reinforcements can be observed for vertical spacing values ranging from $S_{v,c}$ to $S_{v,nc}$. The results indicate that, at least for the reinforcement and fill materials adopted in this study, full interaction between adjacent reinforcements occurred below a reinforcement vertical spacing value of approximately 0.10 m (i.e., $S_{v,c} = 0.10$ m) and no interaction between adjacent reinforcements occurred beyond a reinforcement vertical spacing value of approximately 0.20 m (i.e., $S_{v,nc} = 0.20$ m). Consequently, according to these experimental results, interaction between adjacent reinforcements occurred up to an average distance from active reinforcement (i.e., reinforcement vertical spacing) of 0.15 m from the soil-geosynthetic interface. In Fig. 14, the reinforcement spacing at which a significant change in the interaction between neighboring reinforcements occurred can be used to define the boundary for the composite behavior of a geosynthetic-reinforced soil mass. Specifically, it should be recognized that load in the experimental testing setup was mobilized in only one active reinforcement. In the case of multiple active (i.e., loaded)

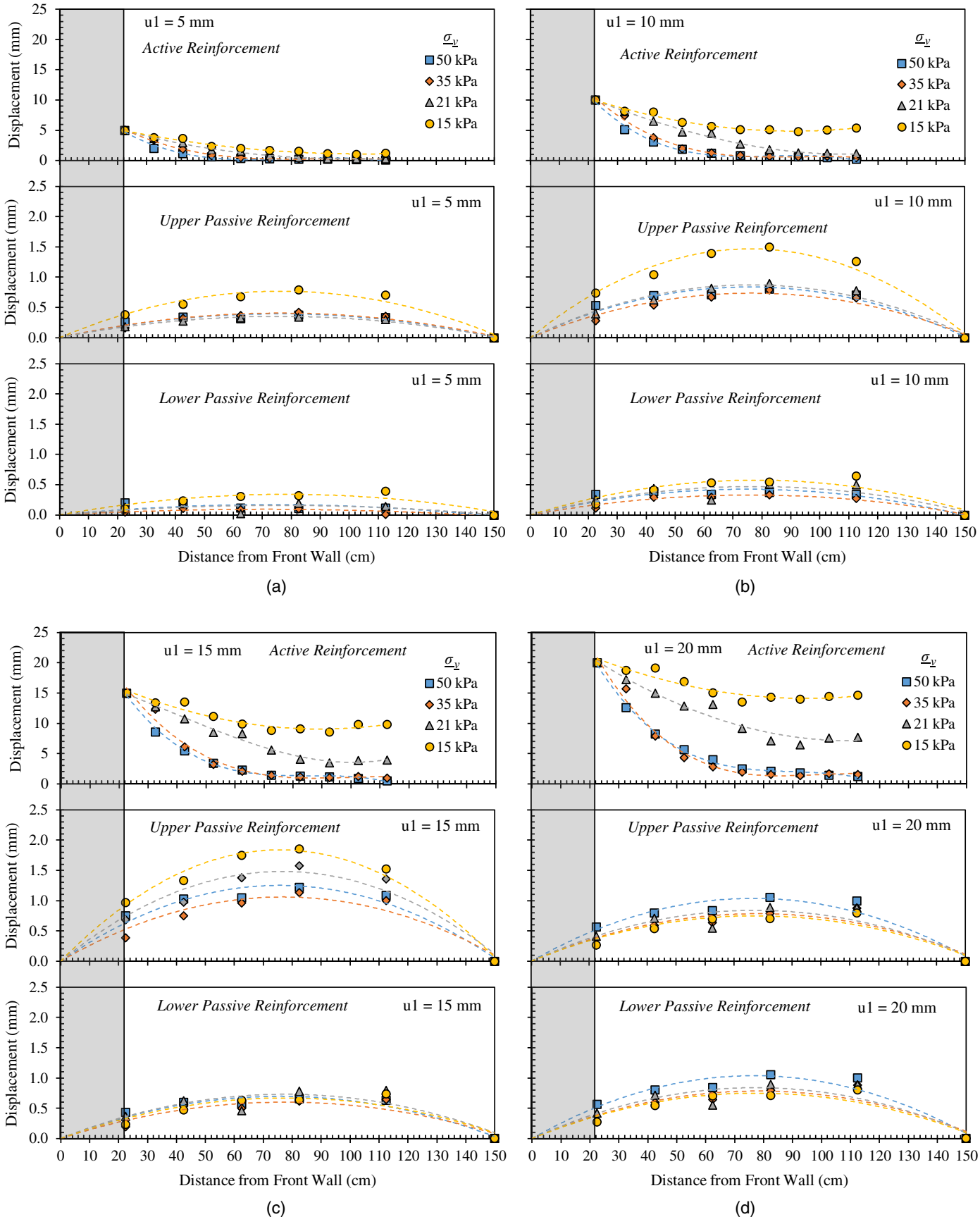

Fig. 9. Reinforcement displacement profiles at various frontal displacements (u1) conducted with $S_v = 0.15$ m: (a) u1 = 5 mm; (b) u1 = 10 mm; (c) u1 = 15 mm; and (d) u1 = 20 mm.

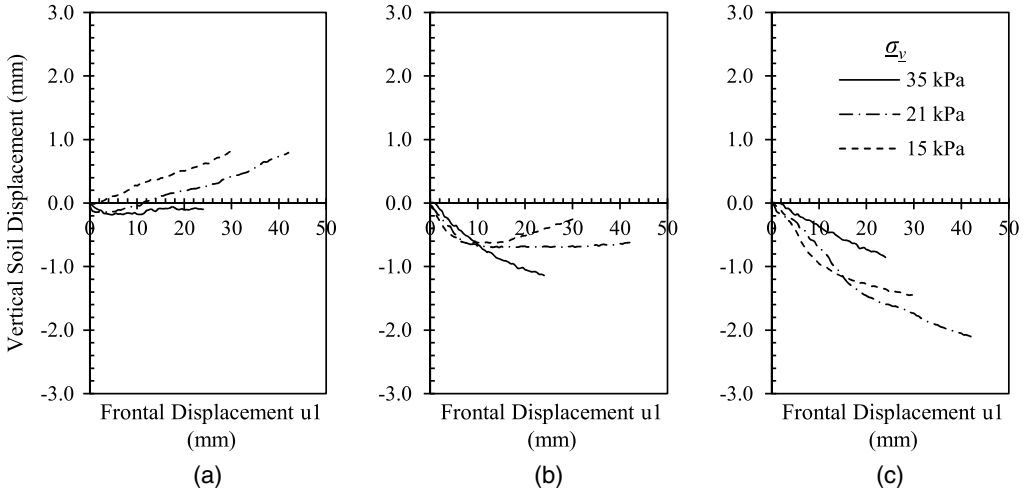

Fig. 10. Vertical soil displacements (measured via artificial gravel particles) relative to frontal displacement at the active reinforcement: (a) front of the soil mass; (b) middle of the soil mass; and (c) back of the soil mass.

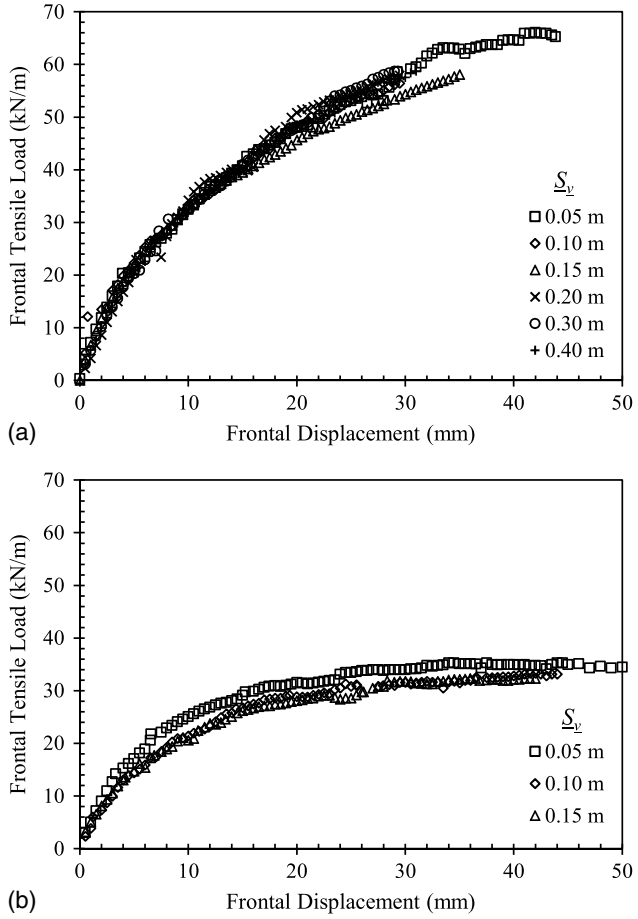

Fig. 11. Frontal tensile load-displacement curves: (a) at normal stress, $\sigma_v = 50$ kPa; and (b) at normal stress, $\sigma_v = 21$ kPa.

reinforcements, the soil in between would be mobilized in shear by the two adjacent reinforcement layers. Consequently, according to these experimental results, composite behavior could be observed for vertical spacing values corresponding to twice the distance from the active reinforcement layer shown in Fig. 14. That is, an average of 0.30 m for select soil (AASHTO No. 8 gravel). This value is in good agreement with current limits for reinforcement spacing established by Adams et al. (2011) for geosynthetic-reinforced soil structures.

Figs. 15(a–d) show the displacement profiles for the active and passive reinforcement layers at testing stages corresponding to active reinforcement frontal displacements (u1) of 5, 10, 15, and 20 mm, respectively, for tests conducted at a normal stress of 50 kPa. The profiles for the active reinforcements show displacements for all tests conducted at the same normal stress. That is, the reinforcement vertical spacing had an insignificant effect on the soil–reinforcement interaction behavior of the active reinforcement. In contrast, the profiles of the passive reinforcements showed higher displacements for tests conducted with reinforcements placed at small vertical spacings compared to those conducted with reinforcements placed at larger spacings. This difference in displacement increased as tensile loading progressed. However, it is notable that no significant difference was observed between the displacements measured for passive reinforcements in tests conducted with reinforcements spaced at 0.05, 0.10, and 0.15 m at a normal stress of 50 kPa. Similar trends were observed in tests conducted with reinforcements spaced at 0.05 and 0.10 m at a normal stress of 21 kPa.

It should be noted that the two passive reinforcements in tests conducted with different reinforcement spacings were subject to different normal stresses due to differences in overburden pressure (i.e., different elevation from the central horizontal plane of the reinforced soil mass). When comparing the loads transferred to passive reinforcements placed at the same elevation in soil masses reinforced at different vertical spacings, the effect of spacing on the interaction among adjacent reinforcements becomes clear. In such a comparison, the soil mass reinforced with closely spaced reinforcements (e.g., S_v) will have more layers than that reinforced with largely spaced reinforcements (twice S_v). In the closely spaced reinforced system, the intermediate reinforcement layers will reduce the interaction between the active reinforcement and passive reinforcement layers placed at the same elevation (i.e., twice S_v from the active layer) as in the largely spaced reinforced system.

Figs. 16(a–d) present the horizontal soil displacements measured for frontal displacements (u1) of 5, 10, 15, and 20 mm, respectively, for tests conducted at a normal stress of 50 kPa. These displacements were measured at specific locations by tracking

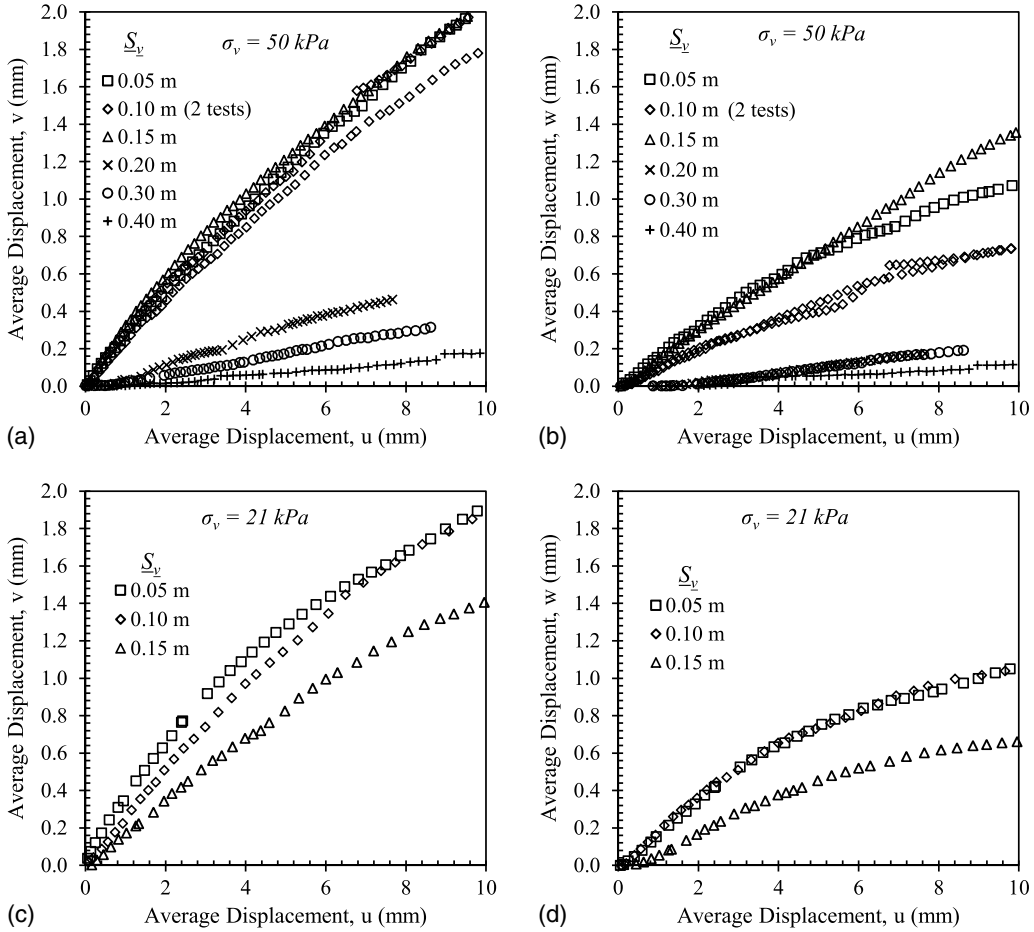

Fig. 12. Average displacements of passive reinforcements relative to average displacements of active reinforcement: (a) upper passive reinforcement ($\sigma_v = 50$ kPa); (b) lower passive reinforcement ($\sigma_v = 50$ kPa); (c) upper passive reinforcement ($\sigma_v = 21$ kPa); and (d) lower passive reinforcement ($\sigma_v = 21$ kPa).

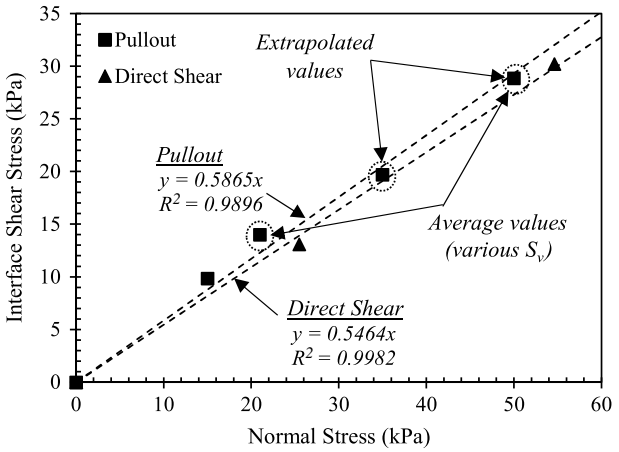

Fig. 13. Soil–reinforcement interface shear strength envelopes (AASHTO Gravel No. 8 and geotextile interface).

artificial gravel particles placed within the soil in a vertical array 30.5 cm from the front wall. The soil adjacent to the reinforcement exhibited a higher rate of displacement due to yielding in the internal shear strength of the fill material, which limited the load transfer from the reinforcement to an area more distant from the reinforcement. Similarly, Figs. 17(a–d) present the horizontal soil displacements measured for frontal displacements (u1) of 5, 10, 15, and 20 mm, respectively, for tests conducted at a normal stress of 21 kPa.

The results indicate that horizontal soil displacements were higher in tests conducted with smaller reinforcement vertical spacings than in tests conducted with larger reinforcement spacings. The active reinforcement conveys the load to the surrounding soil medium, which is then transferred to the passive reinforcements. The soil–reinforcement interfaces of the passive reinforcements have comparatively weaker shear strength than the internal strength of the soil. These weaker interfaces allow the soil between the reinforcement layers to displace more than they would with no passive reinforcements. However, the presence of passive reinforcements resulted in reduced load transfer from the active reinforcement to the soil masses on the other sides of the passive reinforcements.

The active reinforcement in each test conveyed the same load to the surrounding soil because the unit tension of the active reinforcements was found to be unaffected by the reinforcement spacing, as discussed previously. That is, the same energy was conveyed to the soil and passive reinforcements in each test. For tests conducted with reinforcements placed at small vertical spacings, the soil mass between the active and passive reinforcements displaced more compared to tests conducted with reinforcements placed at large vertical spacings, because it received more energy per unit of soil volume

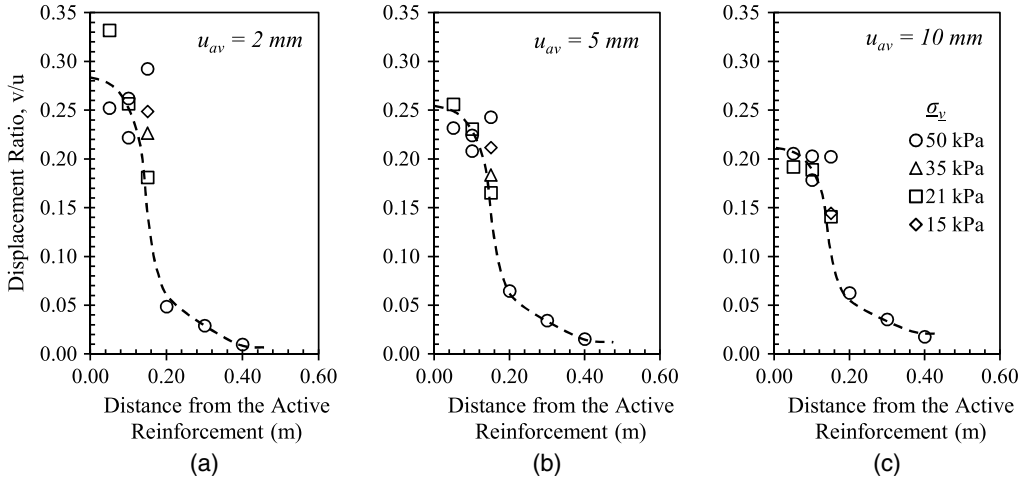

Fig. 14. Average displacement ratio of upper passive reinforcement layers at various average displacements of active reinforcement layers: (a) $u_{av} = 2$ mm; (b) $u_{av} = 5$ mm; and (c) $u_{av} = 10$ mm.

from the active reinforcement. In contrast, the soil masses on the other sides of the passive reinforcements displaced less than in tests conducted with reinforcements placed at small vertical spacings.

Fig. 18 shows the soil–reinforcement relative displacement magnitude at 30.5 cm from the front wall for tests conducted with reinforcements spaced at 0.15, 0.10, and 0.05 m, and confined at normal stresses of 50 and 21 kPa. The relative displacements were obtained by subtracting the reinforcement displacement at this location (i.e., by interpolation between u1 and u2) from the soil displacement measured by the artificial gravel particle adjacent to the reinforcement. The results indicate that the relative displacement at the interface of the active reinforcement was higher in tests conducted at low normal stresses than in tests conducted at high normal stresses. The results in Fig. 18 also reveal a reduction in the soil–reinforcement interface shear stiffness during testing. The results also confirm that the relative displacement was higher in tests conducted with large reinforcement vertical spacings compared to tests conducted with small reinforcement vertical spacings. The displacement of the soil adjacent to the reinforcements was higher in tests conducted with small reinforcement vertical spacings than in tests conducted with large reinforcement vertical spacings. Furthermore, the reinforcement displacement was the same in all tests regardless of the reinforcement vertical spacing. Lastly, Fig. 18 shows the effect of reinforcement vertical spacing on the sensitivity of soil–reinforcement relative displacement to normal stress. No difference in relative displacement was observed in early tensile loading stages between tests conducted at a normal stress of 50 kPa.

Fig. 19 shows the vertical soil displacement measured via artificial gravel particles placed on top of the reinforced soil mass for tests conducted at normal stresses of 50 and 21 kPa, and with reinforcements placed at various vertical spacings. Specifically, Figs. 19(a–c) show the soil displacement relative to the reinforcement frontal displacement of the active reinforcement u1 for the front, middle, and back of the reinforced soil mass, respectively, for tests conducted at 50 kPa. Figs. 19(d–f), by contrast, show the soil displacement for the front, middle, and back of the reinforced soil mass, respectively, for tests conducted at 21 kPa. The results indicate that the soil tended to dilate near the front and settle near the back as tensile loading progressed. The dilation tendency near the front occurred after settlement in early loading stages as shear stresses were generated at the soil–reinforcement interface. The results also show that the dilation tendency was higher in tests conducted with reinforcements placed at small spacings compared to tests conducted with reinforcements placed at large spacings. Additionally, the dilation tendency was high in tests conducted at low normal stresses compared to tests conducted at high normal stresses. That is, the effect of reinforcement vertical spacing on soil–reinforcement interface behavior was more pronounced in tests conducted at a normal stress of 21 kPa.

Conclusions

In this study, a comprehensive testing program was conducted using the soil–geosynthetic interaction experimental approach and equipment developed by Morsy (2017), which were found to be successful in evaluating the interaction among neighboring reinforcement layers. The experimental equipment is not intended to simulate a prototype structure; instead, it is a unit-reinforced soil cell involving an actively loaded reinforcement layer and two adjacent passive reinforcements. Ultimately, the device allows investigating the unevenly loaded contiguous reinforcements. This in turn allows the evaluation of the interaction of multiple loaded reinforcement layers. The equipment parts the interaction of every single reinforcement layer with its neighboring soil and the reinforcement layers from the global reinforced soil system in which all reinforcement layers work together.

The testing program conducted in this study was tailored to evaluate the following aspects: (1) test repeatability, (2) the effect of reinforced soil normal stress, and (3) the effect of reinforcement vertical spacing. The analysis of the experimental results generated in this study led to the following findings:

- The repeatability of the experimental approach adopted for the new soil–geosynthetic interaction equipment was evaluated by conducting tests using two soil–geosynthetic specimens prepared under identical conditions. It was concluded that the testing protocols adopted in this study lead to repeatable results. This was observed by the positive comparison between the results obtained in the two tests regarding the frontal tensile load-displacement curves, the displacement profiles for the active and passive reinforcement layers at various loading stages, and the horizontal soil displacement profiles at various loading stages.
- Evaluation of the frontal tensile load-displacement curves revealed that the resistance of the active reinforcement to frontal tension increases with increasing normal stress and is practically independent of the reinforcement vertical spacing.

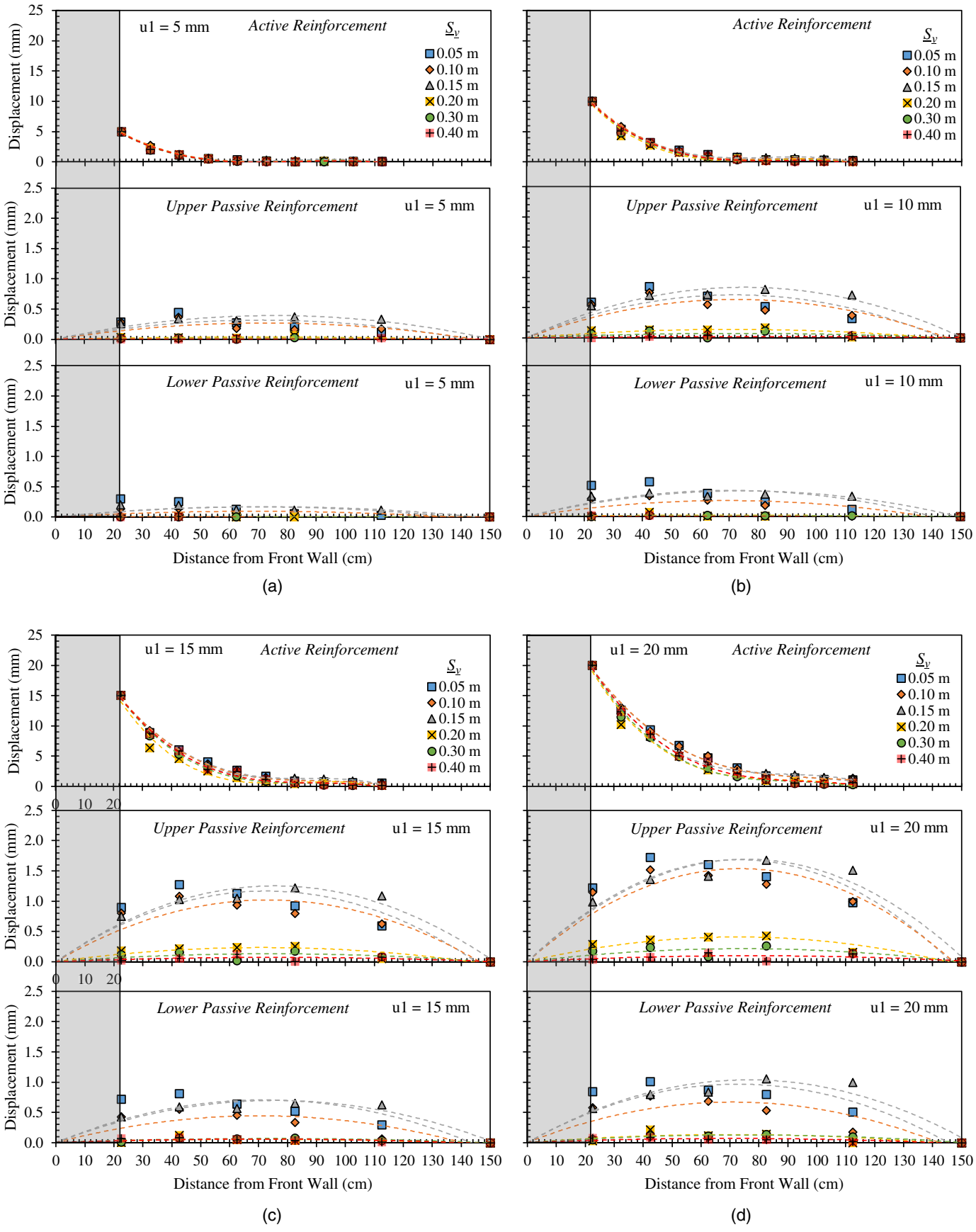

Fig. 15. Reinforcement displacement profiles at various frontal displacements (u1) for tests conducted at $\sigma_v = 50$ kPa: (a) u1 = 5 mm; (b) u1 = 10 mm; (c) u1 = 15 mm; and (d) u1 = 20 mm.

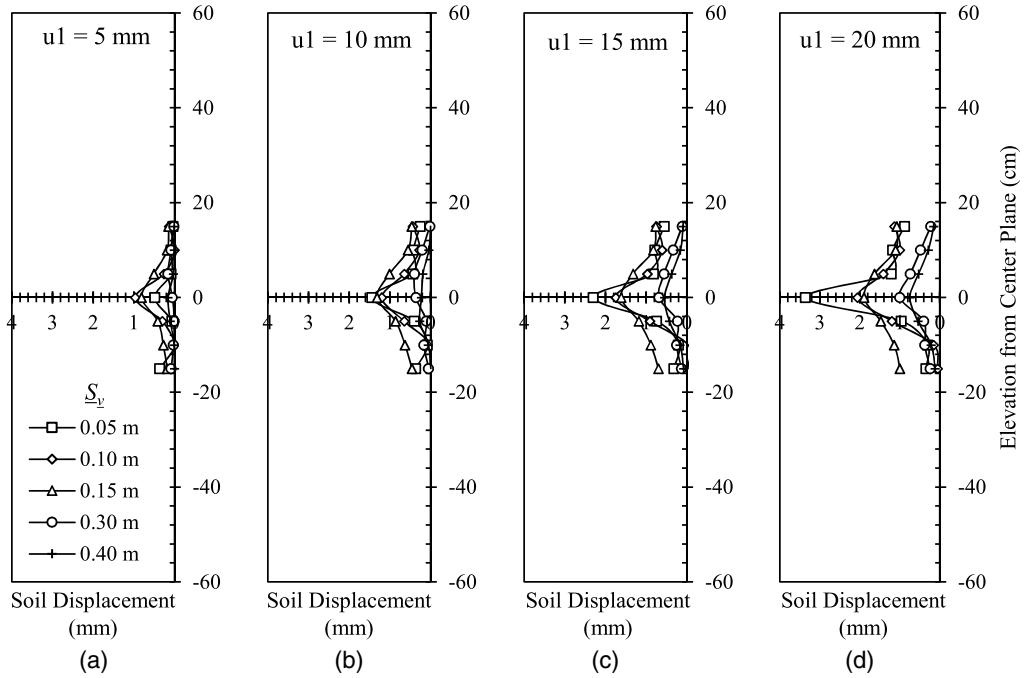

Fig. 16. Horizontal soil displacement profiles (measured via instrumented artificial gravel particles) at various frontal displacements u1 (tests conducted with $\sigma_v = 50$ kPa): (a) u1 = 5 mm; (b) u1 = 10 mm; (c) u1 = 15 mm; and (d) u1 = 20 mm.

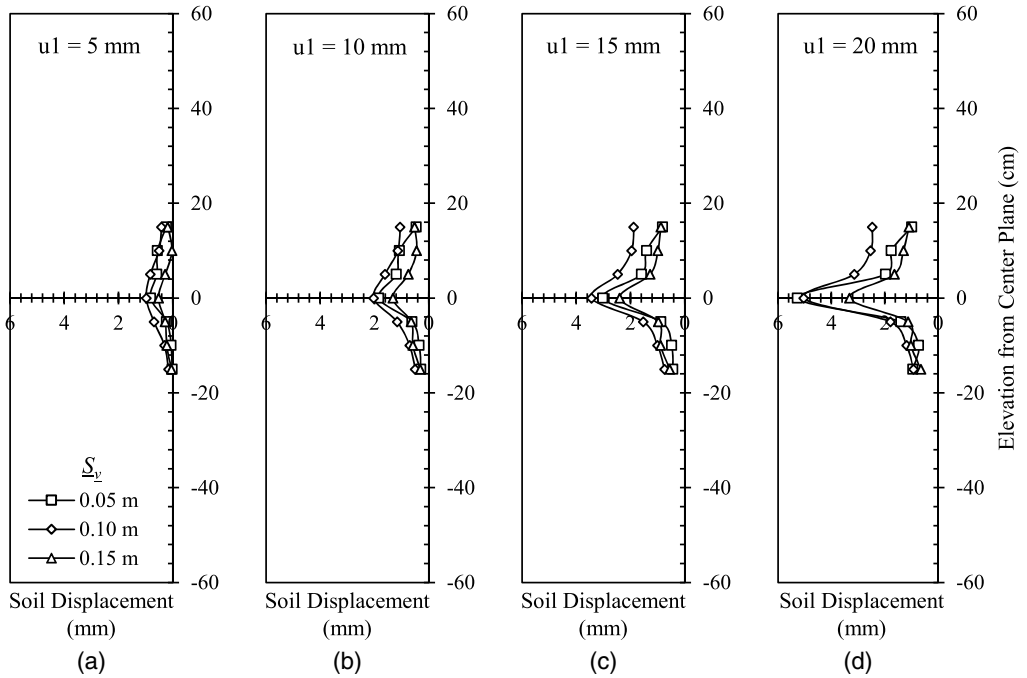

Fig. 17. Horizontal soil displacement profiles (measured via instrumented artificial gravel particles) at various frontal displacements u1 (tests conducted with $\sigma_v = 21$ kPa): (a) u1 = 5 mm; (b) u1 = 10 mm; (c) u1 = 15 mm; and (d) u1 = 20 mm.

- Evaluation of the active reinforcement displacement profiles revealed that the tensile load distribution along the length of the actively loaded reinforcement layer becomes more uniform with decreasing normal stresses and is essentially independent of the reinforcement vertical spacing. Also, the impact of normal stresses on the tensile load distribution was found not to be affected by the reinforcement vertical spacing.
- The effect of normal stress on the interaction between adjacent reinforcements was found to be negligible under load levels consistent with working load conditions. However, the interaction between adjacent reinforcements was found to increase with increasing normal stresses after the interface strength yields, which occurs at earlier loading stages at low normal stress conditions than at high normal stress conditions.

J. Geotech. Geoenviron. Eng., 2019, 145(12): 04019115

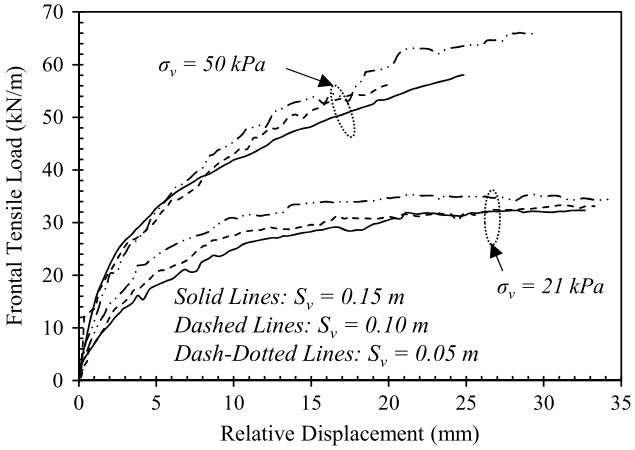

Fig. 18. Soil–reinforcement relative displacement magnitude.

- The magnitude of the lateral soil displacements was found to increase with decreasing reinforcement vertical spacings. This is because adjacent reinforcements (i.e., passive reinforcements) create failure planes at their interfaces that have lower shear strength than the internal shear strength of the soil. These interfaces increased the lateral displacement of the soil layer. However, the presence of the passive reinforcements was found to reduce the load transfer from the active reinforcement to the soil layer located beyond the passive reinforcements. This behavior led to an increased shear stress mobilization in the soil layer between adjacent reinforcements.
- The relative displacements between soil and reinforcement under tension were found to increase with decreasing normal stresses and, in turn, the pullout resistance due to soil–reinforcement interaction. Also, the relative displacements were found to decrease with decreasing reinforcement vertical spacings, which was attributed to the comparatively higher shear stress mobilization in the soil mass between adjacent reinforcements.
- The interaction between adjacent reinforcement layers was found to increase with decreasing reinforcement vertical spacing. A minimum reinforcement vertical spacing threshold was identified, below which the interaction between adjacent reinforcements develops fully. Also identified was a maximum reinforcement vertical spacing threshold beyond which the interaction between adjacent reinforcements is negligible. For the testing program implemented in this study, the minimum and maximum threshold vertical spacings were identified as 0.10 and 0.20 m, respectively. Consequently, according to these experimental results, adjacent reinforcement layers were found to interact when placed at an average distance from active reinforcement of 0.15 m from the soil-geosynthetic interface. That is, in the case of multiple active (i.e., loaded) reinforcements, the soil would be mobilized in shear by the two adjacent

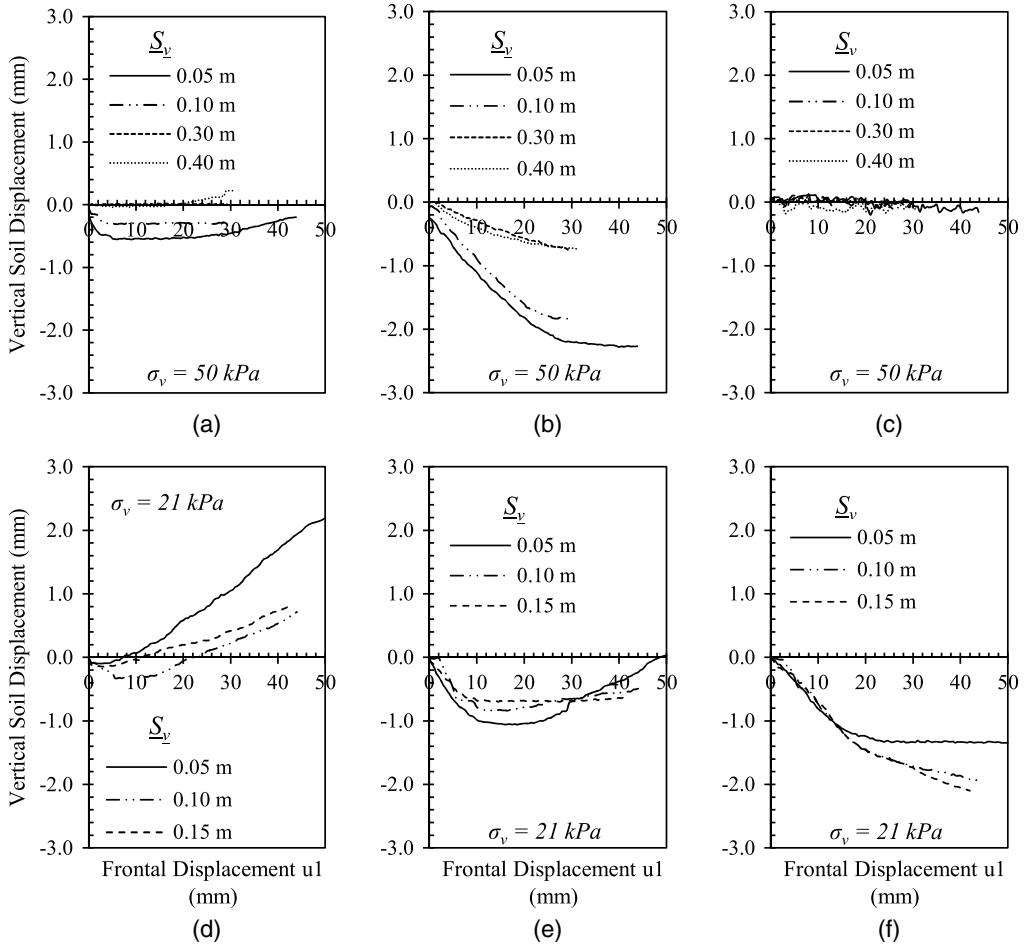

Fig. 19. Vertical soil displacements (measured via artificial gravel particles) relative to frontal displacements at active reinforcement: (a) front of soil mass ($\sigma_v = 50$ kPa); (b) middle of soil mass ($\sigma_v = 50$ kPa); (c) back of soil mass ($\sigma_v = 50$ kPa); (d) front of soil mass ($\sigma_v = 21$ kPa); (e) middle of soil mass ($\sigma_v = 21$ kPa); and (f) back of soil mass ($\sigma_v = 21$ kPa).

reinforcement layers. Accordingly, interaction between adjacent reinforcements could be observed for vertical spacing values corresponding to twice the average distance from the active reinforcement for which interaction occurs. That is, the average vertical spacing for which interaction was found to occur between adjacent reinforcements was found to correspond to 0.30 m for the select soil used in this experimental study.

- Measurement of vertical displacements of the reinforced soil mass revealed that, as testing progressed, the soil tended to dilate toward the front of the active reinforcement and contract toward its back. The magnitude of the dilation was found to increase with decreasing normal stresses and decreasing reinforcement vertical spacing.

Acknowledgments

The work presented in this paper was conducted while the first author pursued his doctoral degree at the University of Texas at Austin, under the supervision of the second author. This research was supported by the National Cooperative Highway Research Program (NCHRP). The opinions presented in this paper are exclusively those of the authors and not necessarily those of the NCHRP. The authors would like to thank Dr. Barry R. Christopher of Christopher Consultants and Dr. Burak F. Tanyu of George Mason University for their contributions to this research.

References

AASHTO. 2017. *Standard specification for classification of soils and soil-aggregate mixtures for highway construction purposes*. AASHTO M145. Washington, DC: AASHTO.

Adams, M., J. Nicks, T. Stabile, J. T. Wu, W. Schlatter, and J. Hartmann. 2011. *Geosynthetic reinforced soil integrated bridge system*. Synthesis Rep. No. FHWA-HRT-11-027. Washington, DC: Federal Highway Administration.

Alshibli, K. A., and S. Sture. 1999. "Sand shear band thickness measurements by digital imaging techniques." *J. Comput. Civ. Eng.* 13 (2): 103–109. https://doi.org/10.1061/(ASCE)0887-3801(1999)13:2(103).

ASTM. 2011. *Standard test method for direct shear test of soils under consolidated drained conditions*. ASTM D3080. West Conshohocken, PA: ASTM.

ASTM. 2014. *Standard test methods for specific gravity of soil solids by water pycnometer*. ASTM D854. West Conshohocken, PA: ASTM.

ASTM. 2016a. *Standard test methods for maximum index density and unit weight of soils using a vibratory table*. ASTM D4253. West Conshohocken, PA: ASTM.

ASTM. 2016b. *Standard test methods for minimum index density and unit weight of soils and calculation of relative density*. ASTM D4254. West Conshohocken, PA: ASTM.

ASTM. 2017a. *Standard practice for classification of soils for engineering purposes (unified soil classification system)*. ASTM D2487. West Conshohocken, PA: ASTM.

ASTM. 2017b. *Standard test method for tensile properties of geotextiles by the wide-width strip method*. ASTM D4595. West Conshohocken, PA: ASTM.

Chen, Y. M., W. P. Cao, and R. P. Chen. 2008. "An experimental investigation of soil arching within basal reinforced and unreinforced piled embankments." *J. Geotext. Geomembr.* 26 (2): 164. https://doi.org/10.1016/j.geotexmem.2007.05.004.

Costa, Y. D., J. G. Zornberg, B. S. Bueno, and C. L. Costa. 2009. "Failure mechanisms in sand over a deep active trapdoor." *J. Geotech. Geoenviron. Eng.* 135 (11): 1741–1753. https://doi.org/10.1061/(ASCE)GT.1943-5606.0000134.

Fannin, R. J., and D. M. Raju. 1993. "On the pullout resistance of geosynthetics." *Can. Geotech. J.* 30 (3): 409–417. https://doi.org/10.1139/t93-036.

Iglesias, G. R., H. H. Einstein, and R. V. Whitman. 2013. "Investigation of soil arching with centrifuge tests." *J. Geotech. Geoenviron. Eng.* 140 (2): 248. https://doi.org/10.1061/(ASCE)GT.1943-5606.0000998.

Jacobs, F., M. Ziegler, and A. Ruiken. 2013. "Experimental investigation of the stress-strain behaviour of geogrid reinforced soil." In *Proc., 2nd African Regional Conf. on Geosynthetics*. Accra, Ghana.

Ketchart, K., and J. T. H. Wu. 2001. *Performance test for geosynthetic-reinforced soil including effects of preloading*. Rep. No. FHWA-RD-01-118. Washington, DC: Federal Highway Administration.

Ketchart, K., and J. T. H. Wu. 2002. "A modified soil–geosynthetic interactive performance test for evaluating deformation behavior of GRS structures." *Geotech. Test. J.* 25 (4): 405–413. https://doi.org/10.1520/GTJ11294J.

Leshchinsky, D., V. Kaliakin, P. Bose, and J. Collin. 1994. "Failure mechanism in geogrid-reinforced segmental walls: Experimental implications." *Soils Found.* 34 (4): 33–41. https://doi.org/10.3208/sandf1972.34.4_33.

Leshchinsky, D., and C. Vulova. 2001. "Numerical investigation of the effects of geosynthetic spacing on failure mechanisms in MSE block walls." *Geosynthetics Int.* 8 (4): 343–365. https://doi.org/10.1680/gein.8.0199.

Morsy, A. M. 2017. "Evaluation of soil-reinforcement composite interaction in geosynthetic-reinforced soil structures." Ph.D. dissertation, Dept. of Civil, Architectural, and Environmental Engineering, Univ. of Texas at Austin.

Morsy, A. M., D. Leshchinsky, and J. G. Zornberg. 2017a. "Effect of reinforcement spacing on the behavior of geosynthetic-reinforced soil." In *Proc., Geotechnical Frontiers 2017*, 112–125. Reston, VA: ASCE.

Morsy, A. M., G. H. Roodi, and J. G. Zornberg. 2018. "Evaluation of soil-reinforcement interface shear band." In *Proc., 11th Int. Conf. on Geosynthetics (11th ICG): Properties and Testing—Reinforcement*, 16–21. Seoul, Republic of Korea: Korean Geosynthetics Society.

Morsy, A. M., J. G. Zornberg, B. R. Christopher, D. Leshchinsky, B. F. Tanyu, and J. Han. 2017b. "Experimental approach to characterize soil-reinforcement composite interaction." In *Proc., 19th Int. Conf. on Soil Mechanics and Geotechnical Engineering (19th ICSMGE)*, 451–454. London, UK: International Society for Soil Mechanics and Geotechnical Engineering.

Morsy, A. M., J. G. Zornberg, J. Han, and D. Leshchinsky. 2019. "New generation of soil–geosynthetic interaction experimentation." *J. Geotext. Geomembr.* https://doi.org/10.1016/j.geotexmem.2019.04.001.

Muhlhaus, H., and I. Vardoulakis. 1987. "The thickness of shear bands in granular materials." *Geotechnique* 3 (37): 271–283.

Palmeira, E. M. 2009. "Soil–geosynthetic interaction: Modelling and analysis." *J. Geotext. Geomembr.* 27 (5): 368–390. https://doi.org/10.1016/j.geotexmem.2009.03.003.

Rui, R., F. van Tol, X. L. Xia, S. van Eekelen, G. Hu, and Y. Y. Xia. 2016. "Evolution of soil arching; 2D DEM simulations." *J. Comput. Geotech.* 73 (Mar): 199–209. https://doi.org/10.1016/j.compgeo.2015.12.006.

Shen, P., J. Han, J. G. Zornberg, A. M. Morsy, D. Leshchinsky, B. F. Tanyu, and C. Xu. 2019. "Two- and three-dimensional numerical analyses of geosynthetic-reinforced soil (GRS) piers." *J. Geotext. Geomembr.* 47 (3): 352–368. https://doi.org/10.1016/j.geotexmem.2019.01.010.

Zhou, J., J. F. Chen, and J. F. Xue. 2012. "Micro-mechanism of the interaction between sand and geogrid transverse ribs." *Geosynthetics Int.* 19 (6): 426–437. https://doi.org/10.1680/gein.12.00028.

Zornberg, J. G., B. R. Christopher, D. Leshchinsky, J. Han, B. F. Tanyu, A. M. Morsy, P. Shen, F. T. Gebremariam, Y. Jiang, and B. Mofarraj. 2019. *Defining the boundary conditions for composite behavior of geosynthetic reinforced soil (GRS) structures*, 997. National Cooperative Highway Research Program (NCHRP), Project 24-41, Washington DC: Transportation Research Board.